STUDY REGARDING THE MODELING AND SIMULATION ON THE INFLUENCE OF AUTOMOBILE BRAKE SYSTEMS ON ACTIVE SAFETY

Marius-Gabriel PATRASCAN[1]

The modeling of the ABS braking system operation has two main components: the mathematical algorithm of car dynamics during braking and the control algorithm that must ensure a implied wheels slip. The mathematical model, "vehicle quarter" of the vehicle dynamics during braking is used in the Matlab program by simulation using Simulink toolbox. There are many possibilities to design a controller, whose control algorithm is to be shown by the on-board computer. Controllers based on artificial intelligence algorithms are used.

Keywords: control algorithm, friction coefficient, slipping coefficient, braking distance, braking time, braking pressure, braking torque, road surface.

1. Introduction

Modern automobiles, especially cars, represent technical systems that are increasingly complex both as structure and operation. The electronic control of the engine operation, as first stage of supervision by the board computer has gradually extended to the main components (transmission, suspension, steering or braking, etc.) to the car as a whole, to itself and to its near and distant environment [4]; all of this was possible due to the embracing of advanced technical solutions based on the principles of automation and telematics. Consequently, the study of modern vehicle dynamics in general, can no longer be restricted to the classical approaches; it is imperative that the movement is addressed systemically, with the means and algorithms of the automatic regulation theory, and of the electronic control and of systems theory [1; 2; 9].

The more stringent requirements on performances of, economy, emissions and safety implied nowadays to cars and the special technological development have led to the need to fit such cars with transducers and elements built-in during fabrication; the emerging of advanced processors and software led completed the background that led to the fitting of cars with complex and advanced electronic control systems of cars [6].

The existence of the board computer and the possibilities of data acquisition and storage allows the performance of a study of vehicle dynamics and

[1] PhD Student, University POLITEHNICA of Bucharest, Romania, e-mail: marius.patrascan@gmail.com

of operation of some systems by using the information provided directly by the built-in elements of the electronic control system (sensors / transducers and building elements/ actuators) [3]. It should be emphasized that nowadays, the cars have many electronically controlled safety systems, many implied on by regulations in force [7]. The aim of this study reffers on modeling and simulation operation of ABS system, on different types of road with different slipping coefficients imposed for ABS system.

2. Modeling and Simulation of ABS Operation

The modeling of ABS operation has two major components: the mathematical algorithm of the car dynamics during braking and the control algorithm which should ensure an implied slipping of the wheels [5; 9].

A mathematical model used in simulation of vehicle dynamics during braking process ("quarter car model") is *Matlab Simulink Toolbox*. Thus, for the *"quarter car"* model, the braking forces and torques are shown in Fig. 1 [3; 5; 8].

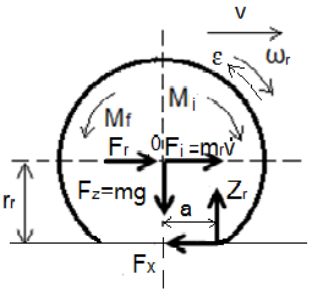

Fig.1. Representation of forces and moments during braking [6].

Fig. 1 shows the movement equations during braking process [8]:

$$\begin{cases} m\dot{v} = -F_x \\ J\dot{\omega}_r = r_r F_x - M_f \end{cases} \quad (1)$$

where $J\dot{\omega}_r = M_i$; m – the mass of the "quarter car" (1/4 of the vehicle weight), v – the longitudinal speed of the vehicle, F_x – the friction force with the runway, J – the moment of inertia, ω_r – the the angular velocity of the wheel, r_r – the radius of the wheel, M_f – the braking moment.

Below, all mathematical formulas [8] are drawn from the movement equations during braking process and will be used in the modeling schema for the simulation of the ABS operation.

The *Fx* force – the friction force induces a moment of the wheel, *Mr*:

$$M_r = F_x r_r \quad (2)$$

Therefore, the second equation from expression (1) becomes:

$$J\dot{\omega}_r = M_r - M_f \quad (3)$$

resulting thus the angular velocity of the wheel:

$$\dot{\omega}_r = \frac{1}{J}\left(M_r - M_f\right) \tag{4}$$

M_f - the braking moment is proportional with the braking pressure, p_f:

$$M_f = k_f p_f \tag{5}$$

Where, k_f is a proportionality coefficient resulted from structural considerations. By these notations, the longitudinal slip a is defined by the expression:

$$a = \frac{v - \omega_r r_r}{v} = \frac{v - v_r}{v} \tag{6}$$

The Matlab Modeling Plan is represented in Fig. 2, used to simulate the operation of *Anti-lock braking system* (ABS). The first differential equation of the model (1) is found in area A at the exit of the modeling block 11, resulting thus the v velocity of the car, whose values are known from block 14 (for subsequent calculations or graphs). In addition, it is found that, at the exit of block 8, the force F_x will result. Integrating the vehicle speed in block 12, we reached the braking space with values known from block 15:

$$S_f = \int_{v_0}^{v_f} v(t)dt \tag{7}$$

where, v_0 *is the initial braking velocity,* and v_f *- the final braking velocity* (it may be NULL or not).

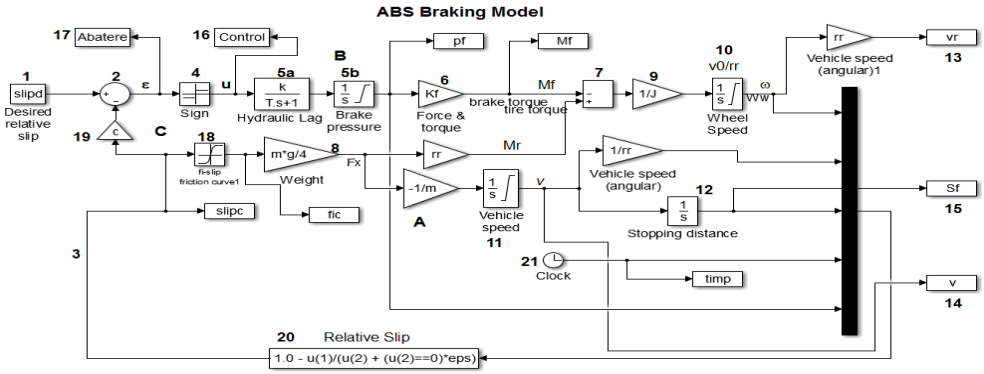

Fig. 2. Modeling plan for the simulation of ABS operation (Matlab).

In area **B** we determine the brake pressure p_f (5a and 5b modeling blocks) and the braking torque M_f (block 6), the latter calculated according to the previous expression (5).

As seen in 5a modeling block, the braking pressure is provided by the master cylinder considered an inertial element of order 1, meaning with the transfer function [8]:

$$W(s) = \frac{k}{Ts + 1} \tag{8}$$

T – the time constant and k - the static transfer coefficient. In addition, the modeling block 5b ensures limitation of the fluids pressure to a maximum value.

The plan also shows that *adder 7* is completed with *the moments* M_f and M_r, the last being calculated with equation (2). At the exit of the adder we reach the difference (M_r -M_f) from the expression (4), which divided by the moment of inertia J results in the values of the derivative ω' - *angular velocity of the wheel* of this expression (at the *exit of the modeling block 9*).

Further on, through integration in the *integrator block 10* (with the initial condition, v_0 / r_r) the wheel angular speed ω_r is reached at the output. Then, the multiplying with r_r can result in the wheel peripheral speed $v_r = \omega_r r_r$, known as *block 13.* Therefore, with the sizes of *the modeling blocks 13* and *14* we can calculate *the slip* with the equation (6). As mentioned, the second largest component of the ABS operation modeling is to establish a slipping control algorithm. This results from the observation that the driver cannot continuously generate a braking torque (by pressing the brake pedal) proper to the grip limit. This is exactly what ABS tends to achieve, meaning the maintaining of a braking moment as close to the gripping moment, resulting in a minimum braking space. In the literature and in practice there are many ways to design a controller, whose control algorithm to be given by the board computer. Thus, classic automatic controls are used (mostly PID: *proportional-integrative-derivative*), controllers based on artificial intelligence algorithms [2]. In the modeling scheme shown in Fig. 2, we used a controller called *"bang-bang" (block 4)*, which is based on the signum function [8], defined for any size *x,* by the expressions:

$$sgn(x) = \begin{cases} 1, \text{ for } x > 0 \\ 0, \text{ for } x = 0 \\ -1, \text{ for } x < 0 \end{cases} \tag{9}$$

In automatic control theory, the *bang-bang controller* switches abruptly between two states; the best known type of controller is *the thermostat ("connected-disconnected")* [6].

As seen from the **C** area, controller 4 has as output, the *u* command, which applies to the area **B** of the hydraulic assembly (offering the values of the braking pressure and the braking torque). The input size of the controller 4 is *error* ε, which is the difference between the slipping implied to ABS (block 1) and the actual slipping durring driving (block 20); obviously the control is perfect if the error is zero ($\varepsilon = 0$).

In Area **C** there is also block 18 that contains the table of values of the gripping coefficient, φ according to slipping *a* for a certain category of road and a

certain state of the same, values known from literature. Other modeling blocks in Fig. 2 fulfill various other roles. For example, block 19 enables switching either on the ABS case ($c = 1$) or, in case of no ABS ($c = 0$). In addition, as noted in the modeling scheme, block 21 counts the time *t.* Below there are some results reached by simulation, considering that the vehicle is moving on a horizontal raceway of dry asphalt-type. As observed in Fig. 3b, it was established that ABS will provide a slip coefficient $a = 0.18$. Very important to mention is that the actual friction coefficient has the most values (97.8%) in the range $\mu_m = 0.6 \div 0.66$ (with an average of 0.62), therefore the ABS system does not work strictly with a_i (a_i=0.18) or with the maximum value μ_{max} ($\mu_{max} = 0.7$).

Fig. 3 shows that the wheels peripheral speed V_r has smaller values than the vehicle speed V_a, which means that indeed there is a slip (shown in Fig. 3b). The graph indicates that there are oscillations of *low amplitude* but of *high frequency* of peripheral wheel speed V_r. It is also noted that *the braking time* is t_f=7.09s, from an initial velocity of the car V_{a0} =170 km/h and up to a final speed V_{af} = 16.22 km/h (final peripheral speed of the wheel, V_{rf} = 13.5 km / h).

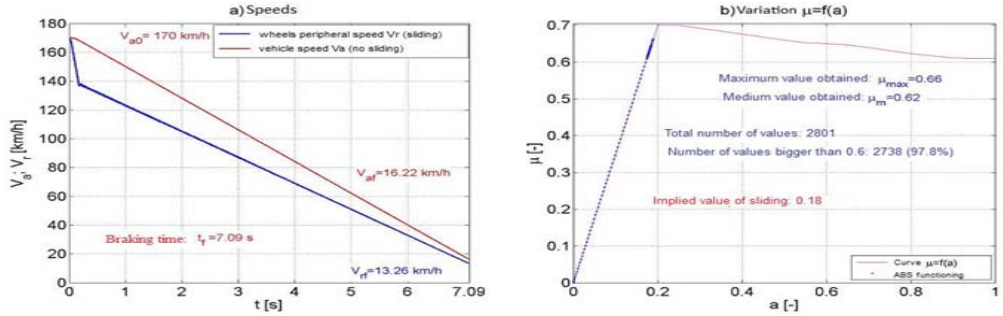

Fig.3. Amplitude oscillations of the wheels peripheral speed, of the car speed according to the braking time and the variation of the friction coefficient according to slipping, a_i=0.18.

Moreover, Fig. 4a shows the time variation of the braking distance S_f, and Fig. 4b shows the braking torque M_f. As seen in Fig. 4a, braking distance value is 185.3m. If we applied the equation known in vehicle dynamics [8], valid for a level road:

$$S_f = -\frac{1}{g}\int_{v_0}^{v_f} \frac{v}{\mu + \frac{kA}{G_a}v^2}dv \tag{10}$$

and considering the average value $\mu_m = 0.62$ in Fig. 3b, then S_f = 181.1m results, a value close to that obtained in Fig. 4a.

Also, if we applied the known equation in vehicles dynamics [8], valid for the braking time:

$$t_f = -\frac{1}{g}\int_{v_0}^{v_f} \frac{1}{\mu + \frac{kA}{G_a}v^2} dv \tag{11}$$

and considering the average value of $\mu_m = 0.62$ in Fig. 3b, then t_f = 7s results, a value close to that obtained in Fig. 3a.

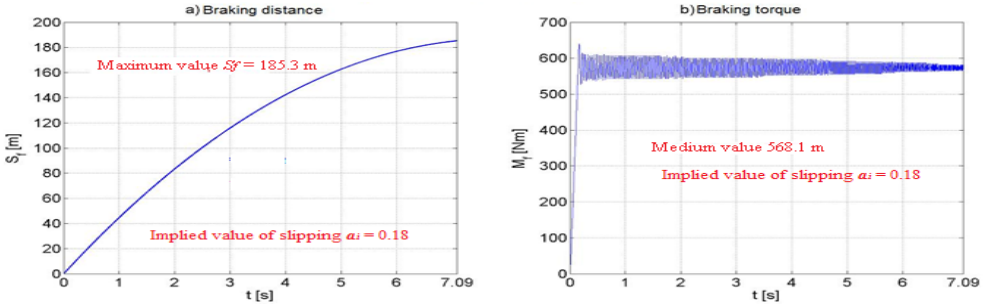

Fig.4. Representation of the braking distance and braking torque in a certain time period, when driving on dry asphalt.

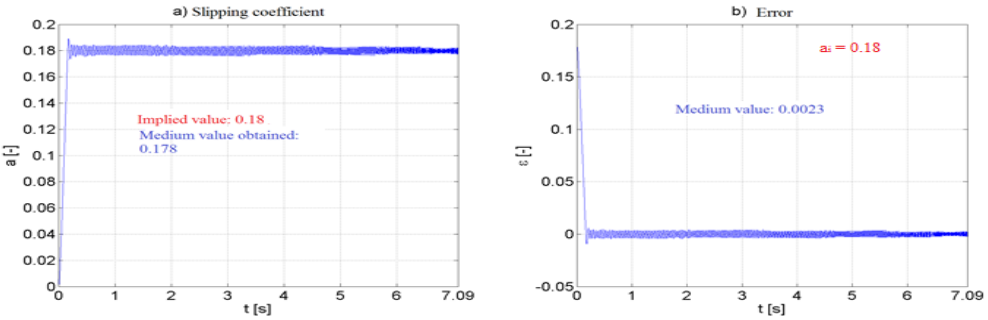

Fig.5. Representation of low amplitude oscillations but with high frequency in ABS operation, a_i = 0,18.

The graphics from Fig. 4b and Fig. 5 confirm the existence of small amplitude oscillations but with high frequency in the ABS function. Fig. 4b shows that the average braking torque is 568.1 Nm. Similarly, Fig. 5a shows that, compared to a value implied for slipping of a_i = 0.18, in the ABS function we obtained an average value of 0.178 (i.e. acceptable deviation). Finally, Fig. 5b shows that, after the start of the ABS, the error between the value implied and the one obtained varies around zero (average 0.0023).

Fig. 6 shows the slipping control algorithm (variation of the command size u), applied by the board computer, and Fig. 7 shows the dependence between the command u and error ε (output and input sizes of the controller 4 in the modeling and simulation scheme shown in Fig. 2).

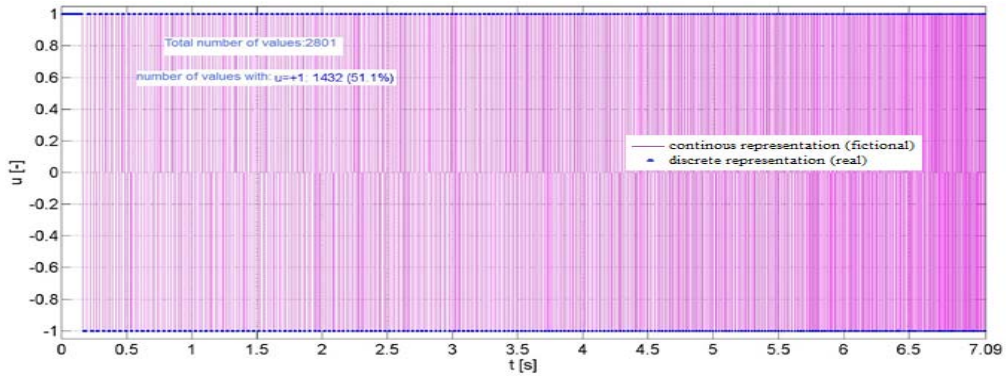

Fig.6. Slipping control algorithm. Variation of u command size according to braking torque, $a_i = 0.18$.

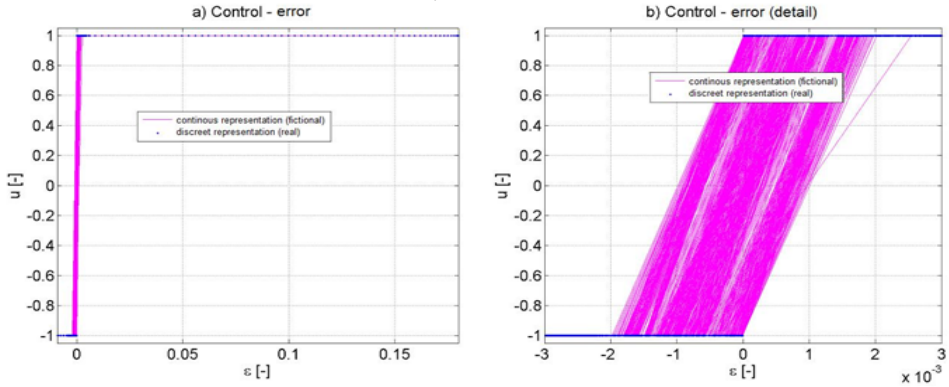

Fig.7. Dependence between the size of the controller output u and the size of the input ε when driving on dry asphalt, $a_i = 0.18$.

Fig. 6 shows also the continuous representation (fictional) and the discrete one, the latter being the real one and showing that the order size has only the values +1 or -1. As observed in the graph, there are several +1 values, because of the beginning of braking, where ABS has some delay in operation (visible in the all graphs).

The graphs in Fig. 7 show that when the error ε between the ABS slipping implied and the actual one reached is negative, the size of the order is $u = -1$, and when error is positive, the size of the order is $u = +1$ (better visible in the detail in Fig. 7b). This example further shows the variation of the braking torque M_f according to the coefficient of slipping a (Fig. 8). Due to oscillations in the sizes variations, the two graphs confirm the existence of a *stable limit cycle* better described in Fig. 8b and Fig. 9.

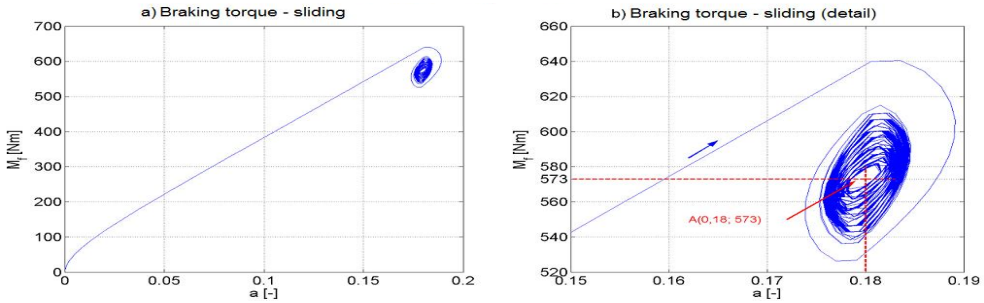

Fig.8. The dependence between the braking torque M_f and slipping coefficient *a,* when driving on dry asphalt, *ai = 0.18*

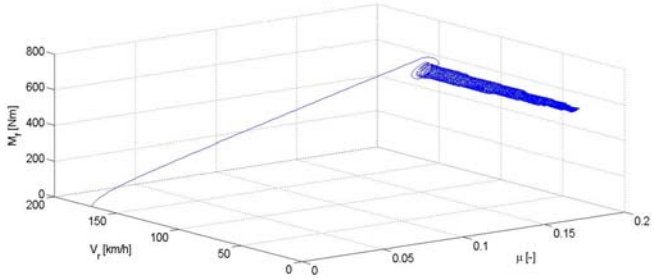

Fig.9. Emphasizing the stable cycle limit $M_f = f(\mu, v_r)$ on a functional ABS, when driving on dry asphalt. Slipping coefficient implied, $a_i = 0.18$.

For the same example, it is believed that a slip larger than the previous one is necessary, respectively $a_i = 0.22$. Thus, we obtained the Fig. 10 graph, similar to Fig. 3. As shown in the graph, this time, the amplitude in oscillations of the wheel peripheral velocity *Vr* is higher than previously, explainable by a higher implied slip, which forces the ABS system to lift the fluid pressure, hence the braking torque, as shown in Fig. 11b (where the average value of 619.3 Nm is higher than the previous one shown in Fig. 4b). This determines the minimizing of the braking space to 171.6m (Fig. 11a), compared to 185.3m in Fig. 4a. In these new conditions, the braking time remains the same, of 7.09s, but the final velocity decrease, as shown in Fig. 10 and Fig. 3a.

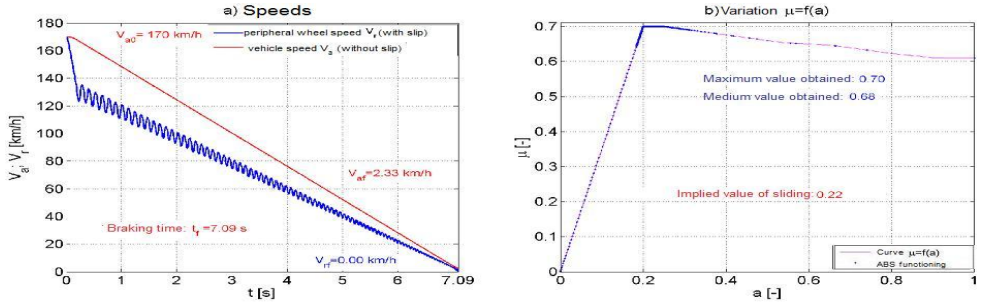

Fig.10. Amplitude in oscillations of the wheels peripheral speed, of the car speed according to the braking time and the variation of the friction coefficient according to slipping, $a_i = 0.22$

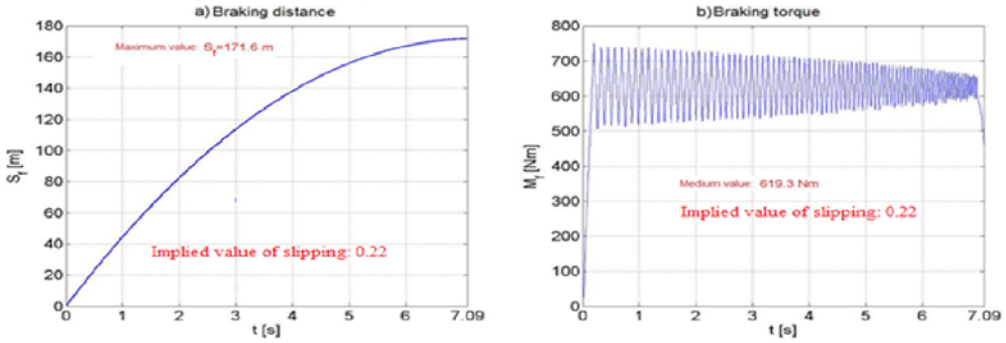

Fig.11. Representation of braking distance and the braking torque when driving on dry asphalt, a_i= 0.22.

Fig. 11b shows that this time, the braking torque falls at the end and predicts a deviation from normal ABS functioning, seen also in Fig. 12a (there is a complete wheel slip, a=1), also confirmed by the existence of a *unstable limit cycle* shown in Fig. 13 (comparable with *stable limit cycle*, Fig. 9).

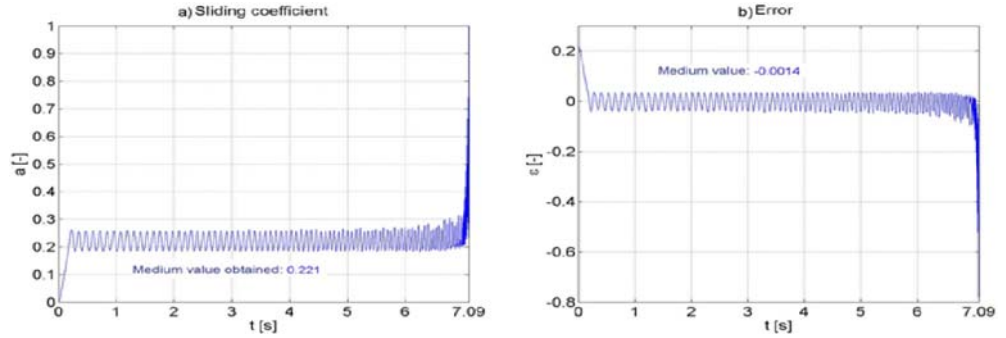

Fig.12. Representation of deviation from ABS system normal operation depending on the average value of the slipping coefficient.

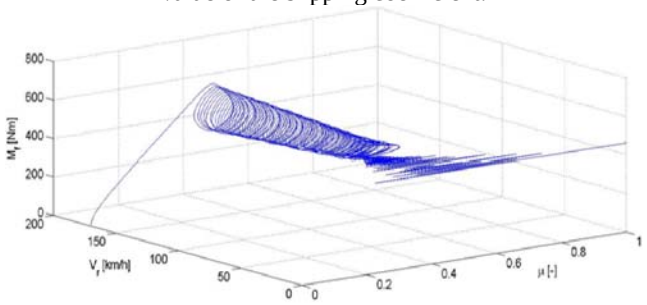

Fig.13. Emphasizing the unstable cycle limit $M_f = f(\mu, v_r)$ on a functional ABS system, when driving on dry asphalt. Slipping coefficient implied, a_i = 0.22.

In the following, we will describe, in a similar manner, results obtained by simulation, considering that the car is moving on a horizontal glazed frost asphalt type. Thus, Fig. 14 shows the values of the speed and of the friction coefficient. In

comparison with Fig. 3 (driving on dry asphalt) it is to be noted that the braking time increased from 7.09s to 16.67s given much lower friction coefficients (Fig. 14b and Fig.3b).

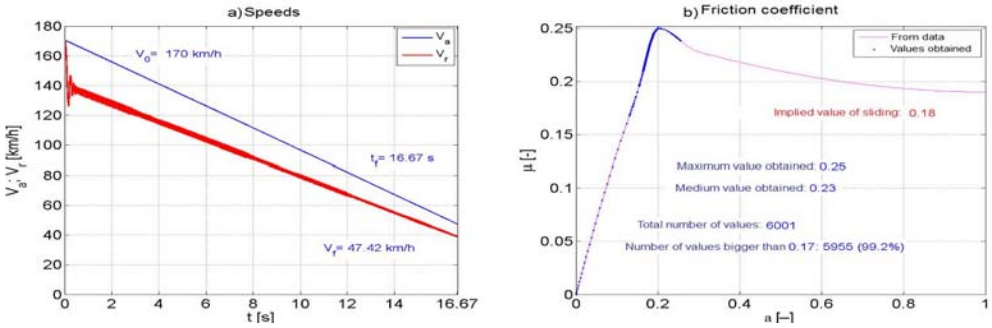

Fig.14. Amplitude in oscillations of the wheels peripheral speed, of the car speed according to the braking time and the variation of the friction coefficient according to slipping, when driving on glazed frost, $a_i = 0.18$.

In these conditions the braking space also increased from 166.4m to 504.9m (comparatively, Fig. 4a and Fig. 15a) obviously with a sensitive decrease in the braking torque, respectively from an average of 567, 8 Nm to 185.4 Nm in the case of glaze (Fig. 4b and Fig. 15b).

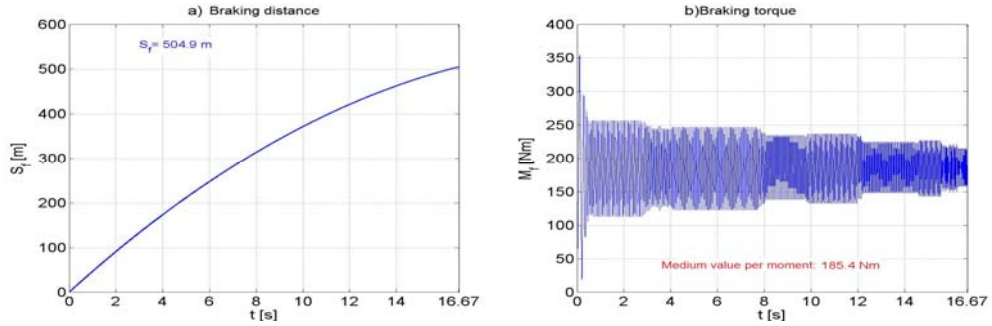

Fig.15. Representation of braking distance and the braking torque driving on glazed frost, depending on the time of braking. Slipping coefficient implied $a_i = 0.18$.

The charts represented show that in case of driving on glaze, there is an increase in the frequency of wheel oscillation, thus leading to the need of frequency analyzing of ABS operation. We can also consider the case when the ABS system is not functional. In this case, the charts from Fig. 16 and Fig. 17 are obtained when driving the car on dry asphalt. Thus, Fig. 16a shows that at the time $t = 0.3$ s the wheel has zero peripheral speed, which means it has a pure slip regime, confirmed also by the value $a = 1$ of the slip coefficient in Fig. 17b. Also, Fig. 3a and Fig. 16a show that the braking time of the car increased from 7.09s to 8.03s, obviously with an increase in braking distance from value 185.3m to 192.3m (shown in Fig. 4a and Fig. 17a).

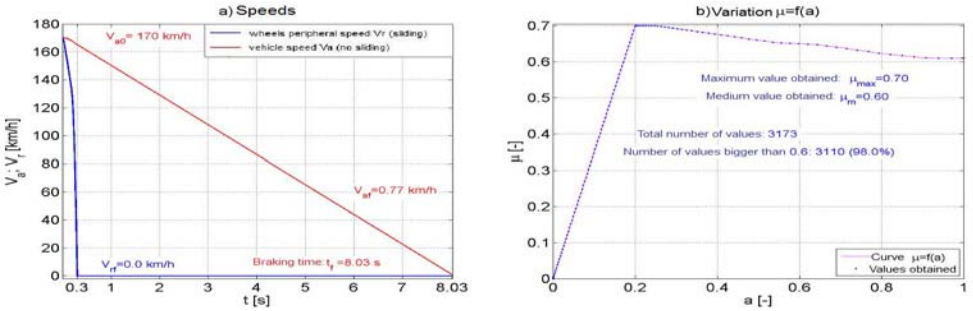

Fig.16. Amplitude in oscillations of the wheels peripheral speed, of the car speed according to the braking time and the variation of the friction coefficient according to slipping, without a functional ABS system.

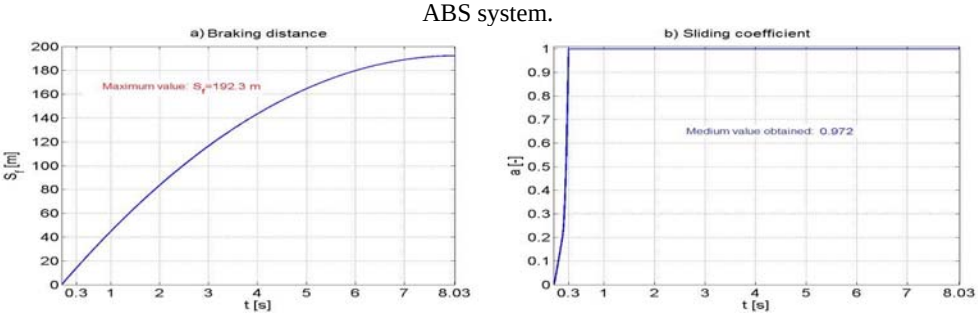

Fig.17. Representation of braking distance and slipping according to braking time, driving on a dry road, without a functional ABS system.

This case is similar to the case in which the ABS is defective, e.g. the pressure modulator does not ensure normal operation of the system. Similarly, such cases can be studied for other types of runways for different slides implied, etc.

3. Conclusions

Table 1 indicates the values reached only for the cases studied in this paper.

Table 1

Two runways and two values of slipping implied to ABS system

Braking time and distance	Dry asphalt a_i=0,18	Dry asphalt a_i=0,22	Dry asphalt without ABS	Glazed frost a_i=0,18	Glazed frost a_i=0,22
t_f [s]	7,09	7,09	8,03	16,67	16,67
S_f [m]	185,3	171,6	192,3	504,9	518,1

According to this table, it is found that when driving on glazed frost the t_f braking time and the t_f braking space substantially increase, compared to the amounts related to the movement on dry asphalt. It also noted that on dry asphalt, the braking time and space are higher in case of inexistence of ABS system (a similar comparison can be made on any runway). The table shows that the braking time remains the same for the two values of slipping imposed a_i, due to the

symmetry compared to the maximum of the friction coefficient curve, but the braking space varies.

On this basis of the above descriptions, other conclusions can also be drawn:
- The existence of transient oscillating processes of the peripheral speed of the wheel, of its slip, its gripping coefficient, timing and brake pressure; towards the end of the braking process, there is decreasing in amplitude and increasing in the oscillations frequency;
- Along with the increase in the wheel slip, there is a change of the oscillating nature by the increase of frequency and the increase of its amplitude; along with the increase in wheel slip, there is also the decrease in brake space; the imposing of more severe requirements to the ABS system results in amplitude decrease and increase of oscillations frequency;
- During ABS operation, there are stable or unstable limit cycles; for the slipping of the wheels implied to ABS system, for which the gripping coefficient is maximum, the lowest values of time and space to brake are reached; on the damp raceways, there is increase in amplitude and frequency of oscillations compared with the dry ones; along with the increase in wheel slip there is also increase in the final value of the speed at which the ABS gets out of operation;
- The existence of transient processes of the peripheral speed of the wheel, of its slip, of gripping coefficient, of brake time and pressure;
- Because, to obtain the lowest values of the braking time and braking distance (which provides traffic safety at the highest level), the ABS system must be imposed a wheel slip corresponding to the maximum of the slip coefficient – gripping coefficient curve, resulting the fact it is advisable that the vehicle is equipped with sensors to estimate the state of the road surface.

R E F E R E N C E S

[1]. *M. Giampiero, M. Ploechl,* Road and off-road Vehicle System Dynamics Handbook, CRC Press, Taylor & Francis Group, London, 2014.
[2]. *E. Marcu, C. Berbente*, UAV fuzzy logic control system stability analysis in the sense of Lyapunov, U.P.B. Sci. Bull., Series D, **Vol. 76**, 2014.
[3]. *C. Jain, R. Abhishek, D. Abhishek*, Linear Control Technique for Anti-Lock Braking System, Int. Journal of Engineering Research and Applications, **Vol. 4**, 2014, pp.104-108.
[4]. *A. P. Stoicescu*, On the maximum braking capability of automobiles, U. P. B. Sci. Bull., Series D, **Vol. 73**, 2011.
[5]. *D. Crolla,* Automotive Engineering, Elsevier Inc., Oxford, 2009.
[6]. *R. Jazar,* Vehicle Dynamics, Springer Science Media, New York, 2008.
[7]. *B. Schofield,* Model-Based Vehicle Dynamics Control for Active Safety, Lund University, Lund, 2008.
[8]. *I. Copae, I. Lespezeanu, C. Cazacu,* Dinamica autovehiculelor (Dynamics of vehicles), Editura ERICOM, Bucuresti, 2006.
[9]. *I. Petersen,* Whell Slip Control in ABS Brakes, Thesis, Norwegian University of Science and Technology, Trondheim, Norway, 2003.